Computational Simulation of an Exhaust Plenum Charged by a Multi-tube Pulsed Detonation Combustor

Maikel Nadolski[1], Mohammad Rezay Haghdoost[2], Kilian Oberleithner[2], and Rupert Klein[1(✉)]

[1] FB Mathematik & Informatik, Freie Universität Berlin, Berlin, Germany
{nadolski,rupert.klein}@math.fu-berlin.de
[2] Laboratory for Flow Instabilities and Dynamics, Institute of Fluid Dynamics and Technical Acoustics, Technische Universität Berlin, Berlin, Germany
mohammad.rezayhaghdoost@campus.tu-berlin.de, oberleithner@tu-berlin.de

Abstract. An efficient computational framework for the numerical simulation of multi-tube pressure-gain combustors for gas turbine applications is introduced. It is based on the open-source AMReX software platform (https://amrex-codes.github.io/amrex/), enhanced to allow for the flexible coupling of multiple computational domains with possibly different dimensionality. Here, six pulsed detonation tubes represented by an efficient one-dimensional model are coupled at their outlets to a threedimensional plenum reservoir. The plenum outlet can be partially blocked to simulate the flow resistance of the first stage of a turbine. This paper presents a validation of this computational setup against measurements obtained from a laboratory experiment with unblocked plenum, and a numerical simulation study of the flow generated by periodic sequential firing of the six detonation tubes into a plenum with a partially blocked exit cross section simulating the flow resistance of a turbine.

Keywords: Multi-domain–multi-dimension CFD · Pressure gain combustion · Pulsed detonation combustors

1 Introduction

Established technology for the most efficient gas turbines relies on combustion via premixed turbulent deflagration. Gas turbine efficiency has been optimized over decades, and even small improvements come at extensive development costs. Pressure gain combustion processes have been identified more recently to bear considerable potential for substantial increases in gas turbine efficiency. In this context, pulsed detonation combustion represents one of the promising alternatives Stathopoulos et al. (2015); Pandey and Debnath (2016).

A pulsed detonation combustor (PDC) operates in a cycle of (i) scavenging and charging, (ii) combustion by an initial deflagration phase followed by deflagration-to-detonation-transition (DDT) and complete burnout by a detonation wave, and

R. King and D. Peitsch (Eds.): AFCC 2021, NNFM 152, pp. 85–102, 2022.
https://doi.org/10.1007/978-3-030-90727-3_6

(iii) expansion of the high-pressure combustion products at the combustor exit. One certain contribution to the expected efficiency gain relative to deflagrative combustion arises from chemical energy conversion occurring at much higher temperatures in the detonation wave as the leading shock of the detonation very strongly compresses the combustible gas prior to chemical heat release. The associated cyclic gasdynamic compression, however, implies a strongly pulsating flow at the combustor exit which can be detrimental for both turbine efficiency and longevity if it were to be received by the turbine in this form.

One approach to controlling the intensity of pulsations received by the turbine consists of inserting an intermediate buffer volume, called the "turbine plenum" or, in short, "plenum" below, in between the combustor exits and the turbine entry plane. Such a plenum will not only disperse the pressure peaks induced by the PDCs but, with a suitable design of combustors, plenum, and their coupling interface, it may also serve as a reservoir that holds a substantially higher mean pressure than the compressor exit pressure. This latter relative pressure gain from compressor exit to turbine plenum may further contribute to the overall engine efficiency if it can be realized without impeding the scavenging of the combustor.

The design of the turbine plenum therefore deserves particular attention, and this is the backdrop of the present study. Motivated by the need to explore different combustor-plenum design combinations, we have developed a flexible and efficient computational framework for related numerical simulations. Its key ingredients are

- an explicit finite volume solver for the compressible Euler equations featuring
- space-time adaptivity,
- generic coupling to reaction kinetics software libraries,
- cut-cell representation of complex domain geometries,
- multi-block domain decomposition, and
- coupling of subdomains with different spatial dimensions.

In previous studies we have validated parts of this computational simulation framework against experimental measurements focusing on the qualitative correctness of coarse-grid simulations (Nadolski et al. 2018), on the detailed representation of shock induced flow structures near the exit of a shock or combustion tube (Rezay Haghdoost et al. 2020a), and on the geometrically more complex case of the flow through a shock divider (Rezay Haghdoost et al. 2020b). Here we aim to validate a simplified model of a PDC combustor implemented within this framework against experimental measurements of a six-tube PDC coupled to an annular plenum as displayed in Fig. 1 (see Rezay Haghdoost et al. 2021, for a detailed description).

Two operation scenarios are considered in this context. In the first scenario, for model validation, only a single combustor is fired. Between two such shots, a long period of scavenging is allowed for, so as to re-establish a quasi-steady inert gas flow through the combustor and the plenum. Only just before the next shot, the inflow stream is charged with fuel over a given time interval, such that about 75% of the tube's length is filled with the desired combustible mixture and the next shot can be fired. The second scenario involves the operation of all

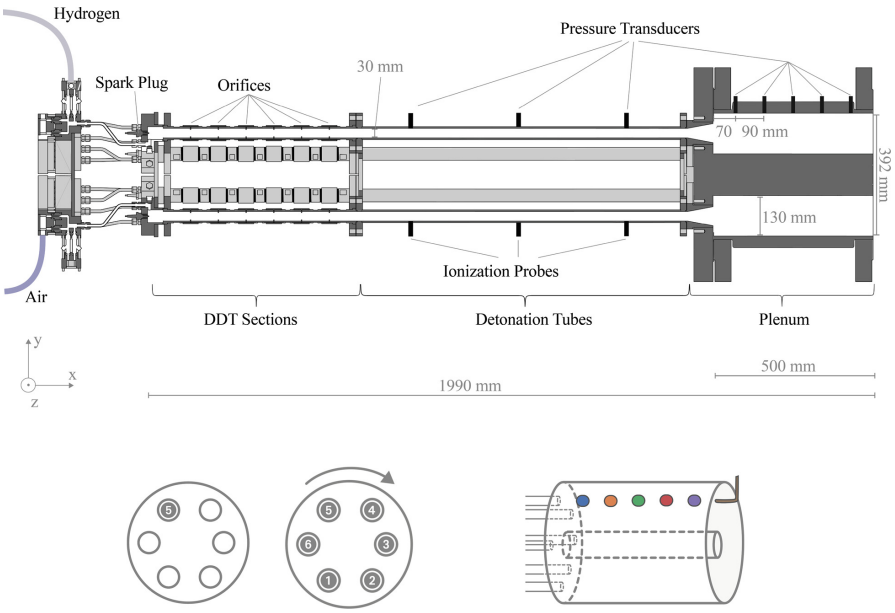

Fig. 1. Top: Test rig for experimental investigations of six pulsed detonation tubes coupled to an annular plenum. The plenum exit can be partially blocked by variable end plates. Bottom right: Sketch of the annular plenum showing the five pressure transducers placed at regular intervals along the plenum wall downstream of the fifth combustor (marked grey in the most left panel). The same color coding of the transducers will be used in later displays of the measured pressure time series. The two panels on the left indicate the two different operating modes (single- and multi-tube operation).

six PDC tubes, which are continuously scavenged by a prescribed fresh air mass flux. The tubes are charged with fuel as in the single-shot experiment, and fired in a continuous sequence one after its previous neighbor in intervals of 10 ms. This scenario is used here for a first computational study of how a relatively large plenum may help to attenuate the extremely strong pulsations induced by the PDC tubes before they reach the plenum exit. An extensive experimental study which includes ion probe measurements within one reference tube (marked grey in the bottom left panel of Fig. 1) to follow the combustion front evolution as well as pressure measurements along this tube and its prolongation into the plenum, though yet without sizeable blocking of the plenum exit, is available in (Rezay Haghdoost et al. 2021).

The realistic simulation of deflagration-to-detonation transition requires the capability to faithfully simulate multi-dimensional turbulent deflagrations in complex geometries, including chemical kinetic effects leading to auto-ignition in flow-induced hot spots and their very local interaction with compression waves (see, e.g., Gamezo et al. 2008; Gray et al. 2017; Bengoechea et al. 2018). As, in this project, we are interested not in these detailed processes within the combustion tube but rather in the impact of the highly dynamic PDC combustor outflow

on the gas dynamics of the plenum, we represent the combustors by simplified one-dimensional models to be described in Sect. 3 below. The free parameters of this model are adjusted to reasonably match the measurements for single-tube firing before we move to a simulation with multi-tube operation of the system.

The remainder of the paper is structured as follows: Sect. 2 provides additional information regarding the numerical simulation system. Section 3 compares the single-tube experiments and computational simulations for validation of the latter. Section 4 presents a first numerical exploration of the effects of increasing blockage of the turbine plenum exit on the gasdynamics of the plenum flow, including a discussion of the possibility of a sustained mean pressure gain across the combustors. Section 5 offers additional discussion and conclusions.

2 Computational Setup

2.1 Extensions of the AMReX CFD Framework

For the implementation of the flow solver, we have adopted the open source software framework AMReX (https://amrex-codes.github.io/amrex/) for patch-wise adaptive structured grid calculations. The development of this platform is spearheaded and maintained by Lawrence Berkeley National Laboratory (LBNL), National Renewable Energy Laboratory (NREL), and Argonne National Laboratory (ANL). The framework provides high-level functionality for the handling of a hierarchy of refined grid patches and for the implementation of highly efficient code that can be dispatched to a variety of high-performance computing architectures.

On this platform we have implemented an explicit second order finite volume compressible Euler solver that uses Strang splitting to account for both multiple space dimensions and chemical reactions. The gasdynamics solver is a MUSCL scheme (van Leer 1979; Munz 1986). It employs the HLLE numerical flux (Einfeldt 1988) with an adaptive utilization of the correction in the advected variables (HLLE(M)) as described by Berndt (2014), and with slope limiting in the characteristic variables. Complex flow domain geometries are accounted for through a variant of the cut-cell technique for use with directional operator splitting as developed in (Klein et al. 2009; Gokhale 2018; Nadolski 2021). The solver is second order in global norms and subject to a reduction to first order at curved solid walls treated by the cut cell scheme.

For the present study, we are interested mainly in efficient simulations of the gas dynamics in the plenum, whereas the details of the combustion process in the PDC chambers are less relevant. It seems justified, therefore, to represent the combustion chambers by quasi-onedimensional simulations, while accounting for three-dimensional effects only for the flow in the turbine plenum. To achieve this within the AMReX framework, we have extended its capabilities accordingly. Prior to our developments, AMReX required the user to fix the number of spatial dimensions for a simulation, and to introduce one large rectangular master mesh that covered the entire flow domain. The computational grid patches on which

the actual calculations were to be carried out had to be placed within – and spatially referenced relative to – this grid super structure.

This principal grid structure has been generalized in this work in two ways. First, we now allow for a general multiblock grid structure so that several rectangular patches may form the basic reference grid. Any two members of this basic structure that touch each other may do so across rather general rectangular subsets of the planes (or lines) forming their surfaces. The second change concerns situations in which the flow on some of these patches can be expected to be approximately uniform in one or more of the cartesian directions. The system now allows for a reduced-dimensional representation of that flow, even though it may couple to a full-dimensional patch somewhere along its surface. The logics of coupling two subdomains with different grid dimensions essentially follows the general adaptive mesh refinement (AMR) strategy in that the lower-dimensional grid patch is treated as a particular coarsened version of an underlying full-dimensional grid of higher resolution. Technical details of these modifications are described in (Nadolski 2021), and the technology has been made publicly available as part the AMReX distribution.

We are thus in a position to simulate the six PDC tubes seen in the experimental setup (Fig. 1) in one space dimension, while pursuing fully three-dimensional simulations of the plenum flow. To avoid too abrupt a change from the one- to the three-dimensional representations, the last 100 mm of the combustor lengths are covered by the three-dimensional grid, so that the coupling interfaces lie in an axial section within which the assumption of a nearly one-dimensional flow in the combustion tubes is still justified. The according computational grid for the domain represented in three space dimensions is shown in Fig. 2, which presents the setup of the computational grid as used in the subsequent simulations, with spacial cell sizes $\Delta x = \Delta y = \Delta z = 1.81\,\text{mm}$.

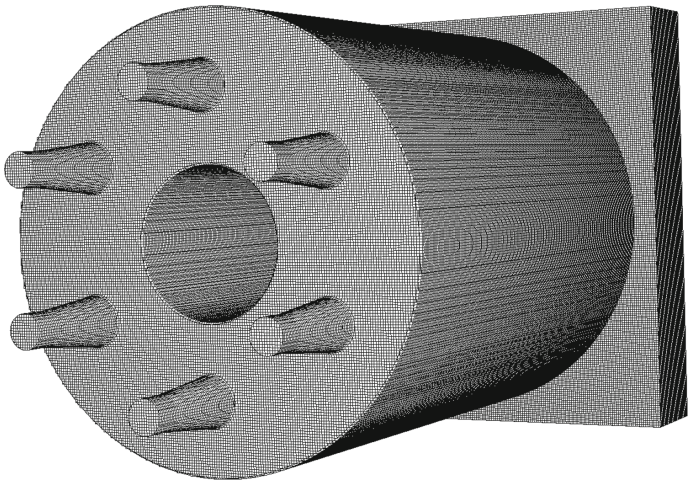

Fig. 2. Grid arrangement for the computational simulation of the gas dynamic processes in the plenum part of the text rig shown in Fig. 1

As we are interested in leading order effects of the gas dynamics in the plenum, we solve the compressible Euler equations for a chemically reacting gas only on the one-dimensional combustor subdomains, while representing the dynamics in the plenum by non-reacting flow with the equation of state obtained from the chemical/thermodynamics library FLAMEMASTER (Pitsch 2021), which is also used for the reactive flow simulation within the onedimensional combustor submodels.

2.2 One-Dimensional Model of the PDC Tube

To avoid the necessity of a detailed, inherently multi-dimensional simulation of deflagration-to-detonation transition (DDT) in the combustors, we utilize a simplified one-dimensional computational model to generate the strong shock outflow into the turbine plenum. This model consists of a one-dimensional computational domain of length L representing the PDC tube (see Fig. 3). At the left end of the tube, the mass flux $\dot{m}$ is prescribed, and this approximates the forced choked inflow applied in the associated experiments in (Rezay Haghdoost et al. 2021) rather well. This mass flux consists of just air or of a stoichiometric hydrogen-air mixture, with equivalence ratio $\phi_{\mathrm{hyd}} = 1.0$. Prior to ignition, the inflow is switched from clean air to the mixture for 26 ms, which leads to a charged length L_{chrg} of the tube of, on average, about 1 100 mm.

The deflagration-to-detonation transition in a real PDC requires a certain run-up distance before the detonation is established. We mimick this process here by a sudden internal energy addition within a width of δx_{ign} centered on location x_{ign}, and by replacing the charged unburnt gas to the left of $x_{\mathrm{ign}} - \frac{1}{2}\delta x_{\mathrm{ign}}$ with burnt gas conditions obtained by constant volume combustion. The local energy addition is modelled by imposing a triangular-shaped temperature profile within this interval with a maximum temperature of T_1 and minimum temperature T_0 as sketched in Fig. 3. This temperature rise occurs at constant density and thus induces a pressure rise and associated strong pressure waves departing to the left and right from the ignition region. It also triggers immediate chemical heat release in the rightward travelling wave wherever the temperature exceeds the ignition threshold of the hydrogen-air mixture. This procedure reproducibly induces the emergence of a detonation wave, and allows us to capture the essential dynamics of the pressure waves that enter the plenum after exiting the PDC chambers.

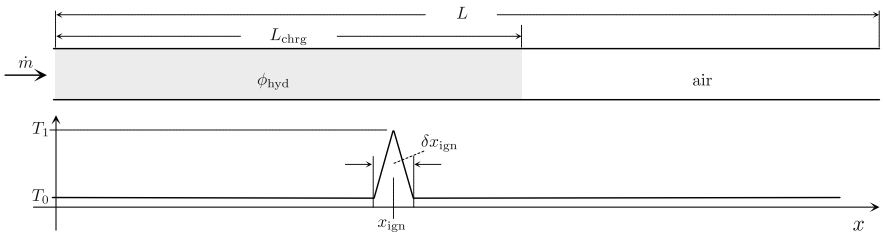

Fig. 3. Sketch of the one-dimensional model of a PDC chamber. $\dot{m}$: mass flux imposed at the entry of the tube; $(L_{\mathrm{chrg}}, \phi_{\mathrm{hyd}})$: length of subdomain charged with hydrogen-air mixture and related equivalence ratio; $(x_{\mathrm{ign}}, \delta x_{\mathrm{ign}}, T_0, T_1)$: center and width of ignition subdomain, minimum and maximum temperatures of the triangular heating profile.

The model's free parameters are, $(\dot{m}, L, L_{\mathrm{chrg}}, x_{\mathrm{ign}}, \delta x_{\mathrm{ign}}, T_0, T_1, \phi_{\mathrm{hyd}})$. For lack of space, we do not present a comprehensive parameter investigation in this paper. Rather, we demonstrate in an exemplary fashion the influence of the inflow mass flux $\dot{m}$ and of the ignition location x_{ign} below, with the other parameters fixed at values that have turned out to yield satisfactory results in a more extensive study (Nadolski 2021), see Table 1.

3 Validation Based on Single-Tube–Single-Shot Tests

For the single-tube–single-shot experiments and numerical simulations, the plenum exit is unblocked and only a single PDC tube out of a total of six is fired. Pressure time series are monitored by the five pressure transducers located on the outer wall of the annular plenum directly downstream of the firing tube at equal spacing (see Fig. 1). The focus is on reproducible single shots separated in time sufficiently to avoid any influence of previous shots on the next one. In a first very straightforwardly implementable series of numerical runs, each simulation is set up separately and with the gas at rest initially. Thus, independence

Table 1. Parameters of the one-dimensional PDC model that are fixed in the present validation study w.r.t. the remaining parameters, i.e., imposed mass flux $\dot{m}$ and hot spot location x_{ign}.

Total PDC tube length	L	1 490	mm
Length of charge	L_{chrg}	1 100	mm
Width of ignition spot	δx_{ign}	50	mm
Lower hot spot temperature	T_0	300	K
Upper hot spot temperature	T_1	2 000	K
Equivalence ratio of charge	ϕ_{hyd}	1.0	

of subsequent shots is guaranteed by construction. In the experiment as well as in the second set of simulations, this independence is achieved by a relatively long scavenging period in between the shots. Although the scavenging flow has a relatively low average Mach number of about Ma = 0.13, we will show below that its influence on the flow in the plenum is substantial, and that the somewhat more elaborate set up of the second simulation series is required to achieve acceptable agreement with the experiment.

Figure 4 shows the results of the pressure measurements. The color coding corresponds to that used to indicate the different pressure transducers in Fig. 1. These measured pressure traces (solid lines) provide the reference for the subsequent numerical sensitivity study (dashed lines).

The simulations that generated the two columns of results in Fig. 4 differ in terms of the imposed mass flux $\dot{m}$ (see Fig. 3). For the left column, the gas was at rest initially, i.e., $\dot{m} = 0$, whereas for the right column, the same mass flux as measured in the experiment was imposed and before charging and firing a shot we let the system settle into a nearly steady state. The rows in the figure represent different locations x_{ign} of the hot spot in the tube. If we let $k = 1, 2$ label the rows, then $x_{\mathrm{ign,k}} = (2k - 1) \cdot 100\,\mathrm{mm}$.

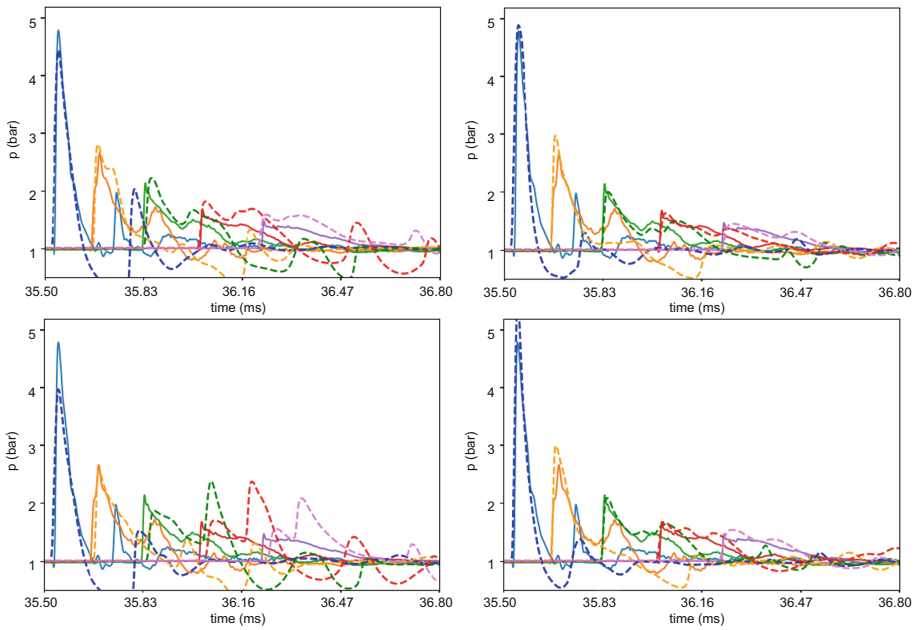

Fig. 4. Measured (solid) and simulated (dashed) pressure traces at the five locations along the plenum wall with color coding as indicated in Fig. 1. Left column: Individual shots into gas at rest; right column: Individual shots into scavenging flow charged for 26 ms before firing, corresponding to a length of the charged gas of approximately 1.1 m. Ignition imposed at $(2k - 1) \cdot 100\,\mathrm{mm}$ for the result shown in the kth row.

The output for experiment and simulations has been shifted along the time axis to guarantee that the first steep pressure rise for the first transducer matches well between the experiment and all the simulations. Both the left and right columns reveal a significant effect of the hot spot location. In the left column (zero initial mass flux), e.g., the pressure trace taken at the fourth transducer location (red dashed curve) develops a strong secondary pulse as x_{ign} increases. This secondary pulse is entirely absent from the solid red line, i.e., from the results of the corresponding measurement. In this sense, the computational signal for hot spot position $x_{\mathrm{ign}} = 0\,\mathrm{mm}$ would seem most promising, were it not for a significant discrepancy in the trace from the first transducer location (blue curves). In fact, both panels on the left show a roughly equal time lag between the simulated first and second maximum of the blue dashed curves, and this time lag is substantially longer than that seen in the experiment. Thus, when the flow is at rest initially a reasonable fit between the measured and simulated pressure traces cannot be achieved by varying the hot spot location alone.

The panels in the right column of Fig. 4, for which the imposed mass flux leads to a Mach number of the scavenging flow of $\mathrm{Ma} \approx 0.13$, do not feature the strong secondary hump in the red (or green) dashed curves as seen in the left column. Thus, this secondary mode is traced back to the absence of a mean flow here. Moreover, the time lag between the first and second pressure maxima of the first transducer (blue curves) shows a clear dependence on the hot spot location. In the second panel the time lag between the maxima agrees very well with that seen in the measurement. Since other features of the traces also agree reasonably well, we take the massflux corresponding to the column on the right and the hot spot location of $x_{\mathrm{ign}} = 300\,\mathrm{mm}$ as the model parameters to be used in the subsequent multi-tube simulations.

The only remaining sizeable discrepancy between the measured and simulated traces concerns the minimum between the first two maxima, which is much lower in the simulations than it is in the measurements. This has been traced back to the way we model the initiation of the detonation wave. In the experiment, an accelerating turbulent deflagration pushes the flow to the transition point, so that the volume in the first part of the tube between tube entry and the establishing detonation is essentially filled with burnt gas at an elevated pressure and the still non-reacting gas in front of the flame has been set in motion by the prior flame-induced gas expansion. In contrast, in the simulation the detonation is triggered by hot spot ignition in a stream of gas that is moving at the nearly constant velocity imposed by the forced inflow mass flux, and the gas between tube entry and ignition location undergoes an instantaneous isochoric reaction. As a consequence, the pre-frontal velocities seen by the emerging detonations as well as the pressures in the respective first sections of the tube differ to some extent between simulation and the experiment. Further improvements of the model readily come to mind but are considered beyond the scope of this paper, because the principal dynamics in the plenum is captured sufficiently well by the present computational setup to enable a first assessment of the dominant gasdynamic effects in the plenum.

4 Multi-tube Firing with Partially Blocked Plenum Exit

Here we pursue a computational simulation study to investigate the response of a multi-tube array of PDC combustors firing in a regular sequence into an annular plenum in analogy with that of the experimental setup of Fig. 1. A partial blockage of the plenum exit simulates the flow resistance of an adjacent turbine (see Fig. 5).

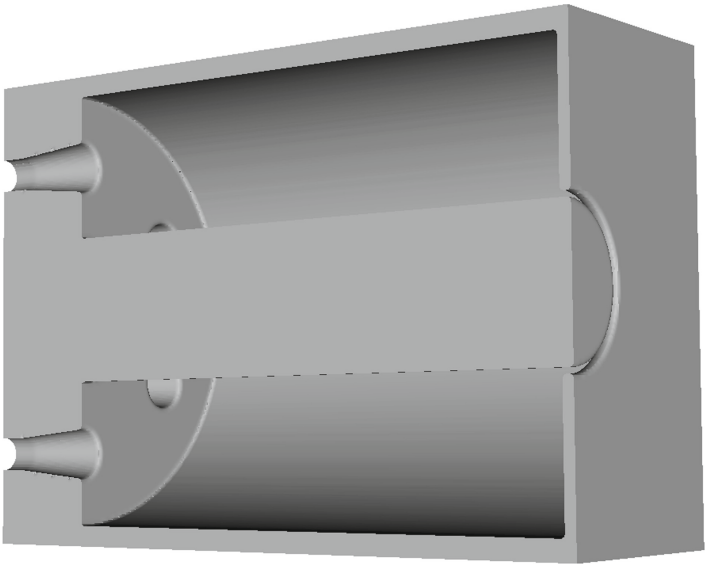

Fig. 5. View of the plenum with a 98% blocked exit mimicking the flow resistance of a turbine.

In this simulation, the six combustors receive a constant imposed mass flux of fresh air or reactive mixture from their entry that induces an average inflow Mach number of Ma = 0.13. One tube fires 10 ms after its next counter-clockwise neighbor, when viewed in the direction of the inflow. Prior to simulating the firing of a tube, it is charged with a stoichiometric hydrogen-air mixture over approximately 1.1 m of its length, corresponding to a time interval of fuel injection of 26 ms, see lower right panel of Fig. 7.

4.1 Plenum Pressure for Forced Inert Gas Flow

A first evaluation concerns the effect of blocking the plenum exit for an inert gas flow generated by imposing the reference mass flux uniformly at the entries of the six combustors. Figure 6 shows pressure traces monitored at the locations of the five pressure transducers in the plenum when the system is started from a medium at rest under ambient conditions and the entry mass flux is imposed

instantaneously at time $t = 0$. After a short time lag, a shock wave arrives at the first transducer, and then the system develops an intense wave activity that leads to the effective mean pressure rise needed to force the incoming mass flux through the remaining crossection of the plenum exit. The left panel in the figure corresponds to a blockage ratio of 96%, while the panel on the right was obtained with the 98% blockage also used for later runs with sequentially firing tubes.

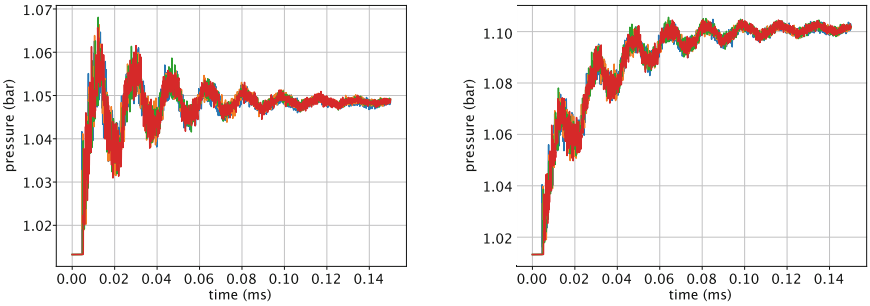

Fig. 6. Increased average plenum pressure needed to force the given mass flux through the partially blocked plenum exit (see Fig. 5). Left: 96% blocking ratio; Right: 98% blocking ratio as used for the multi-tube sequential firing test case.

A similar effect is to be expected in case of reacting flow. Yet, in this case, the chemical heat release will raise temperatures and force the gas to strongly expand. The prescribed mass flux can then pass the plenum exit only if it attains much higher exit flow velocity, and this requires considerably higher excess pressure in the plenum relative to the environment. See also the discussion in the next paragraph.

Table 2. Sequential firing conditions

Firing sequence	next neighbors, clockwise, every 10 ms	
Average length of charge	L_{chrg}	1 100 mm
Charge equivalence ratio	ϕ	1.0

4.2 Mean Plenum Pressure and End-to-End Total Pressure Differences

Here we discuss aspects of the fluid dynamics within the combustors and the downstream plenum under sequential firing conditions. The six tubes are fired one after the other in time intervals of 10 ms. Figure 7 documents the typical cycles of the dynamics within one of the combustors (tube 0) after initial transients have essentially settled. The space-time temperature distribution (top left

panel) reveals that between two shots pressure waves are reflected repeatedly between the forced left and open right ends of the tube. This leads to an approximate equilibration of the pressure and the re-establishment of a nearly stationary scavenging flow.

The bottom right panel of Fig. 7 shows the space-time distribution of the fuel mass fraction. The inflow is charged with fuel over the last 26 ms before the tube is fired. During this time span, the tip of the charge distribution moves to a distance of, on average, 1 100 mm downstream of the tube entry corresponding to a flow velocity of about 42 m/s and a flow Mach number of Ma ≈ 0.13. That is, during the same time span pressure waves can pass about seven times the tube length, and this corroborates our interpretation of the temperature distribution as revealing the approximate pressure equilibration in the tube.

The bottom left panel of Fig. 7 shows the space-time distribution of the axial velocity during the same time period. This distribution not only reveals again the oscillatory nature of the dynamics in between to shots, but it also shows a particularly strong pair of right-running pressure and left-running suction waves right after a shot has been fired. The suction wave is the result of the reflection of the strong detonation-induced shock at the sudden area increase from the end of the tube to the full plenum crossection.

The space-time distribution of pressure (Fig. 7, top right panel), due to the linear scaling of the color code and the extreme pressure spikes arising in the detonation wave, mainly highlights the short time intervals during which the tube is fired and the combustion driven wave passes the length of the tube. To document that our simplified model of the DDT process actually does generate detonation waves, Fig. 8 shows the pressure distributions as a function of space for six output time slices at and after one of the shots in tube 0 at time intervals of 0.2 ms. It is seen how an overdriven detonation, recognizeable by the typical Zel'dovic-von Neumann-Döring (ZND) pressure spike, is generated right after the energy addition (dotted line [with spike at $x \approx -0.975$ m]), that – as long as there is any combustible left – it settles into a mode more akin to a Chapman-Jouguet (CJ) detonation (dashed and long dash-dotted lines), and that it turns into a decaying shock wave towards the right end of the tube (short dash-dotted, solid, and dotted [with spike at $x \approx -0.2$ m] lines).

The same mass flux is forced here through the system as it is in the inert flow case discussed above, but the PDC tubes are now fired sequentially as described in Table 2. The entropy of the burnt gas is considerably larger than that of the inert gas before, so that the burnt gas tends to expand relative to the conditions in the inert flow, and the volume flux through the plenum exit, and hence the exit velocity, increases. This is accompanied by a mean pressure rise as displayed in Fig. 9. Instead of the moderate pressure increase by about 10% for inert gas flow seen in Fig. 6, the pressure now rises above ambient pressure more substantially. Indeed, after the first transient between 50 and 350 ms the remaining effective pressure rise amounts to an increase by about 25%.

Note that this pressure increase arises across then entire system comprising the combustors and the exit plenum. Therefore, a comparably elevated pressure

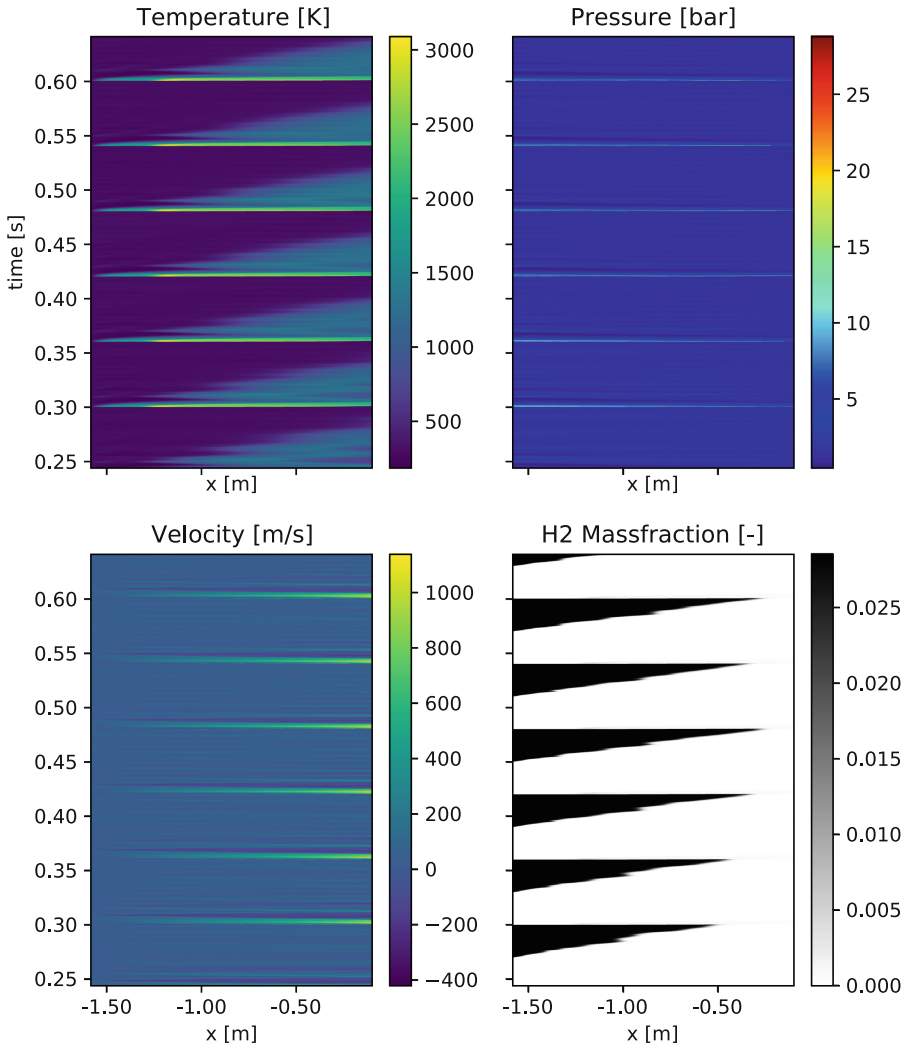

Fig. 7. Space-time traces of the gasdynamics within one of the combustors of the multi-tube configuration.

has to be imposed at the combustor entries to establish the required scavenging flow, and the observed pressure increase does not correspond to a pressure gain from the compressor to the turbine plenum as referred to in the discussion of the second potential efficiency gain in the introduction. To corroborate this, consider the comparison of the time series of area-averaged total pressures at the combustion chamber entry (blue curve) and in the smallest crossection of the plenum exit (orange curve) in Fig. 10. After initial transients have settled, the time and area averaged total pressures at the combustor inlet and plenum

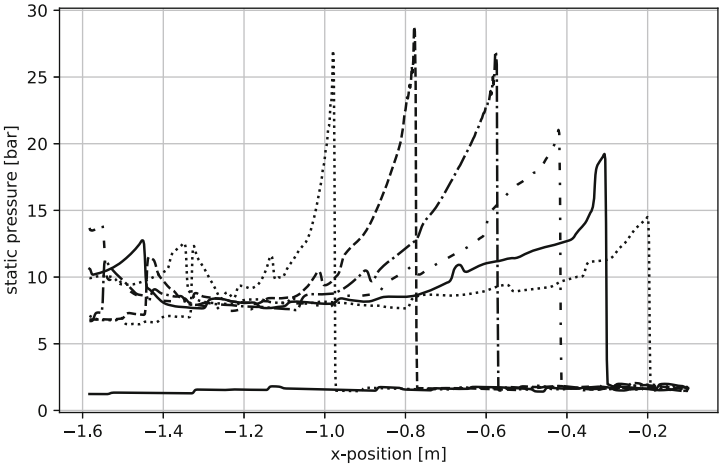

Fig. 8. Snapshots, separated by 0.2 ms, of the spatial pressure distribution in tube 0 shortly after one of its shots. The right-running wave develops first into an overdriven detonation (curve with spike at $x \approx -0.775$ m), then attenuates to a near-CJ detonation mode (spike at $x \approx -0.575$ m), and turns into a decaying shock wave when leaving the fuel-charged region (spike at $x \approx -0.2$ m).

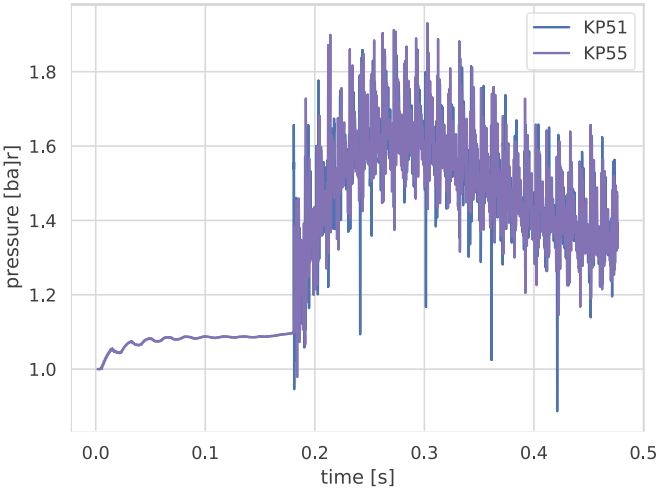

Fig. 9. Pressure traces monitored at the locations of the experimental pressure sensors 1 (KP51) and 5 (KP55) in the plenum (see Fig. 1) under the sequential firing conditions from Table 2.

exit are approximately the same. In fact, realizing an effective pressure gain across a PDC chamber seems impossible if the combustor is to be scavenged by a total volume flux that is comparable to or larger than its own volume, as is the case here. Confer again the bottom right panel of Fig. 7 and its discussion

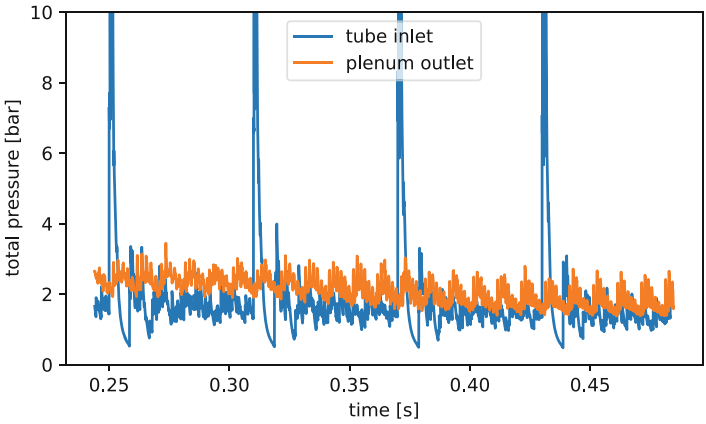

Fig. 10. Time series of area-averaged total pressures at the entry of combustor 0 (left), and within the plenum outlet crossection (right). Note that the total pressure spikes in the combustor reach up and beyond 15 bar. Their traces are truncated in this graph so as to better resolve the fluctuations of much lower amplitude that remain when the pressure pulses directly driven by the chemical heat release have passed.

above. Unless the scavenging flow is close to sonic, pressure waves will oscillate many times across the length of the tube during the scavenging process, leading to an effective pressure equilibration.

A possible remedy could lie in the controlled use of gasdynamic effects involving large amplitude pressure waves in the plenum as realized in studies of the "shockless explosion combustion" (SEC) process (Berndt 2016; Berndt and Klein 2017). An exploration of this idea for PDC applications is beyond the scope of the present work. See, however, (Wolff 2019) for a sketch of a related concept. In any case, even without such a mean pressure rise across the combustors, efficiency gains of a PDC-driven gasturbine relative to a classical turbine with deflagrative combustion should still arise from the first effect mentioned in the introduction, i.e., from chemical reactions occurring at substantially higher temperature in the PDC case.

The turbine plenum's primary purpose is a partial equilibration of pressure to avoid excessive fluctuations of the thermodynamic state and flow velocities within the turbine entry section. Figure 11 shows again the time series of the area-averaged total pressure within the plenum exit crossection (orange) as in Fig. 10, and this is compared here with the time series of the spatial variance of the total pressure in the same crossection. Clearly, the temporal variability of the area-averaged total pressure exceeds the total pressure's spatial variances by a factor of at least two, so that the former provides a good estimate for the total pressure fluctuations in the plenum exit crossection. We conclude, therefore, that the very high pressure spikes induced by detonation combustion, with observed maximum pressures as high as 25 bar, are strongly dispersed within the plenum as intended.

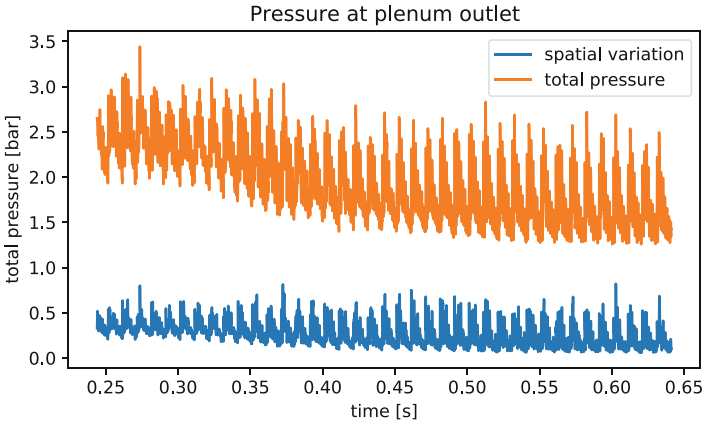

Fig. 11. Time series of the spatial variance of total pressure (blue) and of the total mean pressure (orange) in the smallest crossection of the plenum exit.

5 Conclusions

This manuscript documents the development of an efficient simulation model for multi-tube pulsed-detonation-combustors coupled to a plenum reservoir based on the reactive Euler equations. This system represents the combustion tubes by effective onedimensional models while it provides a fully threedimensional representation of the flow in the plenum. The simulation model has passed validation tests against single-shot experiments within the same geometry.

Simulations with sequential firing of the six combustors with realistic firing frequencies have revealed that the need for substantial scavenging of the tubes between shots leads to pressure equilibration between combustor inlet and plenum. As a consequence, an effective mean pressure rise across the combustors cannot be achieved with this set-up. Alternative designs aiming to overcome this barrier are conceiveable but their study is beyond the scope of the present paper.

The plenum, even though of a relatively simple design that is easy to realize in the experimental context, does succeed in drastically reducing the total pressure variability at the plenum exit (equivalent conceptually to the turbine entry) relative to that at the combustor entries where the full pressure amplitude of the detonation waves is felt. The remaining pressure variability may still be challenging to handle with a standard turbine, so more elaborate designs of the plenum and, particularly, the plenum exit should be investigated in future work.

Aside from the time it takes for a tube to discharge after a shot into the plenum and the pressure to fall back to nearly the compressor pressure, the firing frequency of the current setup is limited by the need to substantially scavenge the combustors between two shots. This is necessary as part of the charge lengths is lost to the less efficient deflagration to detonation transition process. Therefore, and because options of minimizing the DDT-distance are limited, maximization of the efficiency gain promised by detonative combustion requires maximization

of the charge length. When the charge length becomes comparable in magnitude to the entire length of the tube, the scavenging process is dominated by the advection time scale, which then controls the order of magnitude of the maximum firing frequency. This limitation can be overcome only by near sonic scavenging flow which will come, however, with much stronger dissipative losses.

An idea to overcome the second limitation described above, i.e., that with the current setup an effective pressure increase across the detonation tube is not realizeable, has been formulated by Wolff (2019). One might trigger a strong transversally travelling acoustic mode in the plenum be suitable firing sequences of the detonation tubes, and by letting the combustors enter the plenum at a suitable angle. When the phase of low pressure passes by a tube exit, synchronized with the scavenging flow, then the mean (total) pressure in the turbine plenum might still be higher than that at the combustor inlets or in a preceding compressor plenum.

References

Bengoechea, S., Gray, J., Reiss, J., Moeck, J., Paschereit, O., Sesterhenn, J.: Detonation initiation in pipes with a single obstacle for mixtures of hydrogen and oxygen-enriched air. Combust. Flame **198**, 290–304 (2018). https://doi.org/10.1016/j.combustflame.2018.09.017. https://www.sciencedirect.com/science/article/pii/S0010218018304085

Berndt, P.: On the use of the HLL-scheme for the simulation of the multi-species Euler equations. In: Fuhrmann, J., Ohlberger, M., Rohde, C. (eds.) Finite Volumes for Complex Applications VII - Elliptic, Parabolic and Hyperbolic Problems. Springer Proceedings in Mathematics & Statistics, vol. 78, pp. 809–816. Springer, Cham (2014). https://doi.org/10.1007/978-3-319-05591-6_81

Berndt, P.: Mathematical modeling of the shockless explosion combustion. Ph.D. thesis, Freie Universität Berlin, Berlin (2016)

Berndt, P., Klein, R.: Modeling the kinetics of the shockless explosion combustion. Combust. Flame **175**, 16–26 (2017)

Einfeldt, B.: On Godunov-type methods for gas dynamics. SIAM J. Numer. Anal. **25**, 294–318 (1988)

Gamezo, V.N., Ogawa, T., Oran, E.S.: Flame acceleration and DDT in channels with obstacles: effect of obstacle spacing. Combust. Flame **155**(1), 302–315 (2008). https://doi.org/10.1016/j.combustflame.2008.06.004. https://www.sciencedirect.com/science/article/pii/S0010218008001934

Gokhale, N.K.R., Nikiforakis, N.: A dimensionally split cartesian cut cell method for hyperbolic conservation laws. J. Comput. Phys. **364**, 186–208 (2018)

Gray, J., Lemke, M., Reiss, J., Paschereit, C.O., Sesterhenn, J., Moeck, J.P.: A compact shock-focusing geometry for detonation initiation: experiments and adjoint-based variational data assimilation. Combust. Flame **183**, 144–156 (2017). https://doi.org/10.1016/j.combustflame.2017.03.014

Klein, R., Bates, K.R., Nikiforakis, N.: Well-balanced compressible cut-cell simulation of atmospheric flow. Philos. Trans. Royal Soc. Lond. A Math. Phys. Eng. Sci. **367**(1907), 4559–4575 (2009). https://doi.org/10.1098/rsta.2009.0174, http://rsta.royalsocietypublishing.org/content/367/1907/4559. http://rsta.royalsocietypublishing.org/content/367/1907/4559.full.pdf

van Leer, B.: Towards the ultimate conservative difference scheme. J. Comput. Phys. **32**, 101–136 (1979)

Munz, C.D.: On the construction and comparison of two-step schemes for the Euler equations. In: Hirschel, E. (ed.) Notes on Numerical Fluid Mechanics, vol. 14, pp. 195–217. Vieweg Verlag, Braunschweig/Wiesbaden (1986)

Nadolski, M.: Ph.D. thesis, Freie Universität Berlin (2021)

Nadolski, M., Rezay Haghdoost, M., Gray, J., Edgington-Mitchell, D., Oberleithner, K., Klein, R.: Validation of numerical simulations by the exhaust flow of a PDC based high speed Schlieren. In: Notes on Numerical Fluid Mechanics and Multidisciplinary Design: Proceedings of AFCC 2018, vol. 141, pp. 237–253 (2018)

Pandey, K., Debnath, P.: Review on recent advances in pulse detonation engines. J. Combust., 4193034 (2016). https://doi.org/10.1155/2016/4193034

Pitsch, H.: Flamemaster: A C++ computer program for 0d combustion and 1d laminar flame calculations (2021). https://www.itv.rwth-aachen.de/downloads/flamemaster/

Rezay Haghdoost, M., Edington-Mitchell, D., Nadolski, M., Klein, R., Oberleithner, K.: Dynamic evolution of a transient supersonic trailing jet induced by a strong incident shock wave. Phys. Rev. Fluids **5**(073), 401 (2020a)

Rezay Haghdoost, M., et al.: Evaluation of shock dividers using numerical and experimental methods. AIAA J., 2020–0926 (2020b)

Rezay Haghdoost, M., et al.: Mitigation of pressure fluctuations from an array of pulse detonation combustors. J. Eng. Gas Turbines Power **143**(7) (2021). https://doi.org/10.1115/1.4049857

Stathopoulos, P., Vinkeloe, J., Paschereit, C.: Thermodynamic evaluation of constant volume combustion for gasturbine power cycles. In: 11th International Gas Turbine Congress, Tokyo, Japan, pp. 15–20 (2015)

Wolff, S.D.: Entwicklung von fehlererkennungs-, zustandsschätzungs-, regelungs- und ganzzahligen optimalsteuerungsmethoden für pulsierende, detonative brennkammern anhand eines akustischen ersatzsystems. Doctoral thesis, Technische Universität Berlin, Berlin (2019). https://doi.org/10.14279/depositonce-8148